

UNCLASSIFIED

AD NUMBER	
AD324391	
CLASSIFICATION CHANGES	
TO:	UNCLASSIFIED
FROM:	CONFIDENTIAL
LIMITATION CHANGES	
TO: Approved for public release; distribution is unlimited.	
FROM: Distribution authorized to U.S. Gov't. agencies and their contractors; Administrative/Operational Use; JUN 1961. Other requests shall be referred to Wright Laboratory, Air Force Systems Command, Wright-Patterson, AFB, OH 45433.	
AUTHORITY	
15 Sep 1971 per doc. markings, TAB. 71-18; WL/AFSC, IST ltr, 19 Mar 1991	

THIS PAGE IS UNCLASSIFIED

UNCLASSIFIED



AD NUMBER

324 391

CLASSIFICATION CHANGES

TO

FROM

AUTHORITY

WL/AFSC (IST) / 4.

19 MAR 91

THIS PAGE IS UNCLASSIFIED

THIS REPORT HAS BEEN DELIMITED
AND CLEARED FOR PUBLIC RELEASE
UNDER DOD DIRECTIVE 5200.20 AND
NO RESTRICTIONS ARE IMPOSED UPON
ITS USE AND DISCLOSURE.

DISTRIBUTION STATEMENT A

APPROVED FOR PUBLIC RELEASE;
DISTRIBUTION UNLIMITED.

UNCLASSIFIED

AD 324391-L

DEFENSE DOCUMENTATION CENTER
FOR
SCIENTIFIC AND TECHNICAL INFORMATION

CAMERON STATION ALEXANDRIA, VIRGINIA
CLASSIFICATION CHANGED
TO UNCLASSIFIED
FROM CONFIDENTIAL
PER AUTHORITY LISTED IN

TAB. 71-18

15 SEPTEMBER 1971



UNCLASSIFIED

NOTICE: When government or other drawings, specifications or other data are used for any purpose other than in connection with a definitely related government procurement operation, the U. S. Government thereby incurs no responsibility, nor any obligation whatsoever; and the fact that the Government may have formulated, furnished, or in any way supplied the said drawings, specifications, or other data is not to be regarded by implication or otherwise as in any manner licensing the holder or any other person or corporation, or conveying any rights or permission to manufacture, use or sell any patented invention that may in any way be related thereto.

324391

CATALOGED BY ASTIA
AS AD No. _____

XEROX

CONFIDENTIAL

WADD TECHNICAL REPORT 60-328
Supplement 1

(UNCLASSIFIED TITLE)

Flutter Model Tests at Hypersonic Speeds

Flutter Model Tests at Hypersonic Speeds $M = 5$ to 8 Supplement I

Richard P. White, Jr.
John C. Balcerak

CORNELL AERONAUTICAL LABORATORY, INC.

JUNE 1961

DOWNGRADED AT 3 YEAR INTERVALS;
DECLASSIFIED AFTER 12 YEARS.
DOD DIR 5200.10

ASTIA
RECEIVED
JUN 13 1961
TIPDR A

AERONAUTICAL SYSTEMS DIVISION

CONFIDENTIAL

61WRRM-1450 - 57

NOTICES

When Government drawings, specifications, or other data are used for any purpose other than in connection with a definitely related Government procurement operation, the United States Government thereby incurs no responsibility nor any obligation whatsoever; and the fact that the Government may have formulated, furnished, or in any way supplied the said drawings, specifications, or other data, is not to be regarded by implication or otherwise as in any manner licensing the holder or any other person or corporation, or conveying any rights or permission to manufacture, use, or sell any patented invention that may in any way be related thereto.

This document contains information affecting the National defense of the United States within the meaning of the Espionage Laws, Title 18, U.S.C., Sections 793 and 794. Its transmission or the revelation of its contents in any manner to an unauthorized person is prohibited by law.

Qualified requesters may obtain copies of this report from the Armed Services Technical Information Agency, (ASTIA), Arlington Hall Station, Arlington 12, Virginia.

Copies of WADD Technical Reports and Technical Notes should not be returned to the Aeronautical Systems Division unless return is required by security considerations, contractual obligations, or notice on a specific document.

CONFIDENTIAL

WADD TECHNICAL REPORT 60-328
Supplement 1

(UNCLASSIFIED TITLE)

Flutter Model Tests at Hypersonic Speeds
Flutter Model Tests at Hypersonic Speeds $M = 5$ to 8
Supplement I

Richard P. White, Jr.
John C. Balcerak

Cornell Aeronautical Laboratory, Inc.

June 1961

Flight Dynamics Laboratory
Contract No. AF33(616)-6173
Project No. 1370
Task No. 13474

Aeronautical Systems Division
Air Force Systems Command
United States Air Force
Wright-Patterson Air Force Base, Ohio

CONFIDENTIAL

61WWRM-1450

UNCLASSIFIED

FOREWORD

The research project described in this supplementary report was accomplished by the Cornell Aeronautical Laboratory, Inc., Buffalo, New York for the Flight Dynamics Laboratory, Wright Air Development Division, (presently designated Aeronautical Systems Division) Wright-Patterson Air Force Base, Ohio. The work was accomplished under Air Force Contract AF33(616)-6173, Project No. 1370, "Dynamic Problems in Flight Vehicles" and Task No. 13474, "Experimental Investigations of Dynamic Instability Phenomena." Mr. Dale E. Cooley of the Dynamics Branch, Flight Dynamics Laboratory was Task Engineer. This supplementary report presents results for configurations not reported in the main body of this report.

The test phase of the project was conducted by C.A.L. in the E-2 Hypersonic Blowdown Tunnel of the von Karman Facility, Arnold Engineering Development Center, Tullahoma, Tennessee.

Since the flutter data presented herein were obtained for configurations in the Mach number range $5 \leq M \leq 8$, the title of this supplement is slightly different from that of the main report which included data for the Mach number range 5 to 7.

This document, excepting the title, is classified CONFIDENTIAL because it contains experimental flutter data in the hypersonic speed regime which can be employed to determine design criteria for the prevention of flutter of lifting surfaces for future hypersonic flight vehicles.

UNCLASSIFIED

ABSTRACT

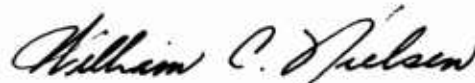
Experimental flutter data are presented in the Mach number range of $5 \leq M \leq 8$ for configurations supplementary to those for which data is presented in the basic report. The results of correlative analyses to determine the accuracy and applicability of piston theory in predicting the aeroelastic instability of these configurations in this speed range are also included.

A total of thirty-two semirigid (roll-pitch) flutter data points were obtained during the experimental phase of the program to determine the effects of Mach number, aspect ratio, leading-edge bluntness and thickness on flutter.

PUBLICATION REVIEW

This report has been reviewed and is approved.

FOR THE COMMANDER:



WILLIAM C. NIELSEN
Colonel USAF
Chief, Flight Dynamics Laboratory

WADD TR 60-328, Suppl. 1

CONFIDENTIAL

SUMMARY

This supplement to WADD TR 60-328, Ref. 1, describes a theoretical and experimental flutter program that was conducted in the hypersonic speed regime to determine the effects of Mach number, aspect ratio, leading-edge bluntness and thickness on the flutter characteristics of unswept, semirigid, half-span models. The models tested were dynamically similar to the model described in the basic report except for the systematic variations made to investigate the above effects on the flutter characteristics. Experimental results in terms of a flutter velocity index, $V/b \omega_p \sqrt{\mu}$, and frequency ratio, ω_f/ω_p , vs. Mach number and frequency ratio, ω_r/ω_p , are presented for the semirigid models which were tested in the Mach number range of $5 \leq M \leq 8$. Theoretical flutter analyses, both neglecting and including the measured amounts of structural damping, were conducted for most of the model configurations.

The main results obtained indicate the following:

1. Over the frequency ratio range tested at $M \cong 6$ the basic $R = \frac{1}{2}$ model appears to be slightly more stable than the basic $R = 1$ model.
2. The effect of blunting the leading edge of the basic modified double wedge profile model at $M \cong 6$ is stabilizing over the frequency ratio range covered.
3. The effects of increasing thickness were found to be destabilizing at the Mach numbers tested. Piston theory predictions of the effects of thickness were found to be conservative at a thickness ratio of 8% whereas they closely predicted the flutter velocity index at thickness ratios of 4 and 6%.
4. For all the frequency ratios tested, on both the $R = \frac{1}{2}$ model and the $R = 1$ blunt nose model, there is a destabilizing trend in the range $6 < M < 7$, and the start of a stabilizing trend apparent at $M = 8$. It appears that the amount of destabilization between $M = 6$ and 7 and the amount of stabilization at $M = 8$ are dependent to some extent on frequency ratio. Piston theory does not adequately predict these variations of flutter velocity index with Mach number.
5. The predicted values of flutter frequency ratio, $(\frac{\omega_f}{\omega_p})$, using piston theory were generally greater than the experimental values when structural damping was not included in the analyses, but the correlation was generally improved when structural damping was included.

WADD TR 60-328, Suppl. 1

UNCLASSIFIED

TABLE OF CONTENTS

<u>Section</u>		<u>Page</u>
I.	INTRODUCTION.....	1
II.	DESCRIPTION OF MODELS AND EQUIPMENT.....	2
III.	PRELIMINARY TESTS.....	3
IV.	WIND TUNNEL TESTS.....	3
V.	FLUTTER ANALYSES.....	3
VI.	DISCUSSION OF RESULTS.....	4
VII.	CONCLUSIONS AND RECOMMENDATIONS.....	10
VIII.	REFERENCES.....	12

WADD TR 60-328, Suppl. 1

UNCLASSIFIED

UNCLASSIFIED

LIST OF ILLUSTRATIONS

<u>Figure</u>		<u>Page</u>
1	Measured Coupled Mode Node Lines and Frequencies, Semirigid Models.	20
2	Test Section Mach Number vs. Stagnation Pressure.	23
3	ω_F/ω_P and $V/b\omega_P\sqrt{\mu}$ vs. ω_R/ω_P , $R = \frac{1}{2}$ Model, Mach No. $\cong 6.0$	24
4	ω_F/ω_P and $V/b\omega_P\sqrt{\mu}$ vs. Mach Number, $R = \frac{1}{2}$ Model, $\omega_R/\omega_P = 0.514$	25
5	ω_F/ω_P and $V/b\omega_P\sqrt{\mu}$ vs. Mach Number, $R = \frac{1}{2}$ Model, $\omega_R/\omega_P = 0.544$	26
6	ω_F/ω_P and $V/b\omega_P\sqrt{\mu}$ vs. Mach Number, $R = \frac{1}{2}$ Model, $\omega_R/\omega_P = 0.670$	27
7	$[V/b\omega_P\sqrt{\mu}]_{\text{EXP}}/[V/b\omega_P\sqrt{\mu}]_{\text{CALC}}$ vs. Mach Number for Various Frequency Ratios, $R = \frac{1}{2}$ Model.	28
8	ω_F/ω_P and $V/b\omega_P\sqrt{\mu}$ vs. ω_R/ω_P , Blunt Nose Model, Mach No. $\cong 6.0$	29
9	ω_F/ω_P and $V/b\omega_P\sqrt{\mu}$ vs. Mach Number for Various Frequency Ratios, Blunt Nose Model.	30
10	ω_F/ω_P and $V/b\omega_P\sqrt{\mu}$ vs. Thickness Ratio, Mach No. $\cong 5.0$	31
11	ω_F/ω_P and $V/b\omega_P\sqrt{\mu}$ vs. Thickness Ratio, Mach No. $\cong 6.0$	32
12	ω_F/ω_P and $V/b\omega_P\sqrt{\mu}$ vs. Mach Number for Various Thickness Ratios, $\omega_R/\omega_P \cong 0.50$	33

WADD TR 60-328, Suppl. 1

UNCLASSIFIED

LIST OF TABLES

<u>Table</u>		<u>Page</u>
I	Summary of Nondimensional Model Parameters.	13
II	Pitch Inertia of Suspension System for the Semirigid Model Configurations.	14
III	Mass Properties of Semirigid Models	15
IV	Summary of Zero Airspeed Vibration Test Results	16
V	Summary of Wind Tunnel Test Results	17
VI	Summary of Calculated Flutter Results	18
VII	Comparison of Calculated and Experimental Flutter Results	19

WADD TR 60-328, Suppl. 1

UNCLASSIFIED

LIST OF SYMBOLS

R	Aspect ratio of semispan
b	Model semichord, inches
c	Model chord, inches
g	Acceleration due to gravity, in./sec. ²
g_R	Structural damping coefficient of uncoupled roll mode, nondimensional
g_P	Structural damping coefficient of uncoupled pitch mode, nondimensional
I_R	Roll inertia of semirigid models, lb.-in.-sec. ²
I_P	Total mass moment of inertia in pitch of semirigid models, lb.-in.-sec. ²
l	Model semispan, inches
P_0	Absolute tunnel stagnation pressure, lb./in. ²
r_P	Radius of gyration in pitch nondimensionalized by the semichord
t	Maximum model thickness, in.
T_0	Tunnel stagnation temperature, °R
t/c	Maximum thickness-to-chord ratio of airfoil; nondimensional
V	Velocity in test section, ft./sec.
x_0	Distance from the leading edge to pitch axis nondimensionalized by the chord
x_P	Distance from the pitch axis to the center-of-gravity nondimensionalized by the chord
μ	Nondimensional wing density ratio, $= \frac{m'}{4b^2}$

WADD TR 60-328, Suppl. 1

UNCLASSIFIED

ρ	Density of air in test section, lb.-sec. ² /in. ⁴
ω_F	Flutter frequency, rad./sec.
ω_P	Frequency of uncoupled pitch mode for semirigid models, rad./sec.
ω_R	Frequency of uncoupled roll mode for semirigid models, rad./sec.
β	$= \sqrt{M^2 - 1}$
P.A.	Pitch-axis
C.G.	Center-of-gravity
m'	Equivalent mass per unit span of semirigid models, lb.-sec. ² /in. ² = $\frac{3 I_R}{l^3}$

UNCLASSIFIED

I. INTRODUCTION

WADD TR 60-328 (Ref. 1) describes a theoretical and experimental flutter program that was conducted in the hypersonic speed regime to determine the effects of Mach number, frequency ratio, center-of-gravity location, pitch-axis location, mass ratio, radius of gyration and thickness on the flutter characteristics of a semispan model having a modified double wedge profile and a square planform. Due to the importance and general interest of the results obtained, a WADD report, Ref. 1 was written to disseminate the information quickly. The present supplementary report presents results of subsequent tests in the Mach number range $5 \leq M \leq 8$, that were performed to determine the effects of aspect ratio, leading-edge bluntness, thickness, and Mach number on the flutter characteristics of the basic models.

Manuscript released by the authors on 1 February 1961 for publication as a WADD Technical Report.

WADD TR 60-328, Suppl. 1

UNCLASSIFIED

II. DESCRIPTION OF MODELS AND EQUIPMENT

A. MODELS

The models used during this supplementary test program were all of the semirigid type, restrained at the root by springs in roll and pitch.

The basic semirigid model was the same as that used in the tests discussed in the main body of this report (Ref. 1) and had the following nondimensional parameters:

Maximum thickness-to-chord ratio, $t/c = 0.04$

Elastic axis at 40% chord, $x_o = 0.40$

Center-of-gravity at 50% chord, $x_p = 0.10$

Radius of gyration, $r_p = \sqrt{0.30}$

Uncoupled roll-pitch frequency ratio, $\omega_R/\omega_P = 0.50$

Half-span aspect ratio = 1

Profile: Modified double wedge, fore and aft wedge lengths = 18.3% chord

The various model test configurations are identified by letter and number designations, i.e., SR-20-9. The SR designation identifies the model as semirigid. The first number signifies a particular configuration, while the second denotes a model number. Table I presents a list of the model configurations and their corresponding parameters.

B. EQUIPMENT

The suspension and instrumentation systems were those discussed in detail in Ref. 1. The pitch inertia of the suspension system for each semirigid configuration is listed in Table II. The roll inertia of the suspension system is negligible with respect to that of the model.

WADD TR 60-328, Suppl. 1

UNCLASSIFIED

III. PRELIMINARY TESTS

The mass properties of the semirigid models listed in Table III were obtained prior to wind tunnel testing in the same manner as described in Ref. 1. A summary of the zero airspeed vibration test results obtained prior to each flutter test are listed in Table IV and the first and second mode node lines are presented in Figure 1.

IV. WIND TUNNEL TESTS

The wind tunnel tests were performed in the E-2 tunnel at the von Karman Facility, AEDC, Tullahoma, Tennessee. The E-2 tunnel is presently capable of operating at Mach numbers of 5, 6, 7, and 8. The tunnel has been recalibrated because of changes made to the tunnel throat subsequent to the tests reported in Ref. 1, and the new plots of Mach number vs. P_0 are shown in Figure 2.

During the test program two nonflutter data points were obtained at $M = 8$ for $P_0 = 1420$ and 1550 psia. The tunnel is calibrated only up to a P_0 of 1000 psia at $M = 8$. It is believed that the Mach number at these higher pressures is that at a P_0 of 1000 to within $\pm 2\%$. This Mach number, therefore, was considered to be the Mach number for these higher pressures.

For this series of tests, a flow alignment check was made at $M = 8$, and the test results indicated that no flow alignment difficulties would be encountered for models having the designed roll stiffness. Large amounts of model rolling due to a small degree of flow misalignment were encountered at $M = 6$ with the blunt nose model, however, when roll stiffnesses much lower than those anticipated had to be used in order to obtain flutter.

Of the thirty-two data points, four were obtained at stagnation temperatures slightly below the liquefaction temperature. These are identified in Table V which summarizes the wind tunnel test results. The effects on the flutter data of operating slightly below the liquefaction temperature are believed to be negligible for the reasons given in Ref. (1).

V. FLUTTER ANALYSES

Except for the blunt nose models, flutter analyses were conducted for all configurations using the third-order piston theory described in Ref. 2. The calculations were made both assuming zero damping, and also including the amounts of structural damping measured on the models. A listing of the calculated results is given in Table VI and a comparison of the calculated and experimental results is given in Table VII.

CONFIDENTIAL

VI. DISCUSSION OF RESULTS

A. FLUTTER RESULTS FOR $R = \frac{1}{2}$ MODEL

1. Effect of Frequency Ratio Variation for $R = \frac{1}{2}$ Model

The effects of variation in frequency ratio on the flutter characteristics of the $R = \frac{1}{2}$ model at $M = 6$, are shown in Fig. 3. The experimental flutter velocity index obtained with an $R = 1$ model having essentially the same basic nondimensional flutter parameters, (Ref. 1), have also been shown in this figure for purposes of comparison. Also shown are results of piston theory analyses for the $R = \frac{1}{2}$ model assuming (1) zero structural damping and (2) the amounts of structural damping measured on the models. The interesting features of the results obtained at a nominal Mach number of 6 for the $R = \frac{1}{2}$ model are:

- a. Over the frequency ratio range for which comparison data were obtained the variation of the flutter velocity index with frequency ratio follows essentially the same trend as that obtained with the $R = 1$ model.
- b. Based on the experimental data obtained, the effects of decreasing the aspect ratio from unity to one-half appears to be slightly stabilizing over the frequency ratio range covered.

While flutter results were not obtained for the $R = \frac{1}{2}$ model below a frequency ratio, $\omega_R / \omega_p = 0.49$, the similar trends of the flutter velocity index between the $R = 1$ and $R = \frac{1}{2}$ models over the frequency ratio ranges tested indicates that the $R = \frac{1}{2}$ model might have the same rapid rise in the flutter velocity index with decreasing frequency ratio as that obtained with the $R = 1$ model. Results reported in Ref. 1 for the $R = 1$ models indicated that the reason for the more rapid rise of the flutter velocity index with decreasing frequency ratio than that predicted by theoretical results was probably due to the center-of-pressure location being further aft than that predicted by the theory.

The apparent stabilizing effect due to reduction of the aspect ratio from unity to one-half seems opposite to the effect found at $M = 3$ for a model having essentially the same profile and nondimensional flutter parameters (Ref. 3). In Ref. 3, a slight destabilizing effect was noted as the aspect ratio was reduced from 1.0 to 0.50. The reason given in Ref. 3 for this reduction was that the Mach cone emanating from the tip of a wing with an aspect ratio of 0.50 covers a substantial portion of the total wing area at $M = 3$. In the Mach cone region the aerodynamic center is moved forward and the influence of such a forward shift is destabilizing.

WADD TR 60-328, Suppl. 1

CONFIDENTIAL

On the basis of only the hypersonic similarity parameter, βR , where $\beta = \sqrt{M^2 - 1}$, it might be deduced that the results obtained at $M = 6$ should also show that decreasing the aspect ratio is destabilizing. The reasoning behind this deduction is as follows: For a model having a given aspect ratio, βR decreases with decreasing Mach number. The data presented in Ref.'s 1 and 3 indicates that as the Mach number decreases from 6 to 3, there is a destabilizing trend of the flutter velocity index. Thus a decreasing value of βR can be associated with a destabilizing trend of the flutter velocity index. Since, at a given Mach number, βR also decreases with decreasing aspect ratio, it might be expected that the flutter velocity index would also decrease.

There are other aerodynamic effects, however, which are not accounted for by this hypersonic similarity parameter. For example, the viscous effect of the boundary layer, which might override the destabilizing effects predicted by the hypersonic similarity parameter βR . Although the actual reason for the slight stabilizing effect that was found at $M = 6$ as the aspect ratio was decreased from unity to one-half is not fully understood based on the information studied, it appears that some other effects not investigated during this program might have caused this unexpected trend. Further investigations in this area are needed to better explain this effect of aspect ratio.

2. Effect of Mach Number Variation for the $R = \frac{1}{2}$ Model

Figures 4 through 6 present the data collected for three different frequency ratios to show the effects of Mach number on the flutter velocity index. The data show that frequency ratio has a pronounced effect on the variation of $V/b\omega_p\sqrt{\mu}$ with Mach number. Also included in Figs. 4 through 6 are the theoretical results calculated with and without the inclusion of the effects of structural damping.

Figure 4 shows the effect of Mach number on the flutter characteristics of the $R = \frac{1}{2}$ model having a frequency ratio, $\omega_R/\omega_p = 0.514$. Experimental results were obtained only at $M = 6, 7$ and 8 for this model since the air supply available at the time was not sufficient for testing at $M = 5$. The flutter motion obtained at a Mach number of 6 was of a different nature from that obtained at Mach numbers of 7 and 8. At $M = 6$, the flutter was of a rapidly divergent type while at $M = 7$ and 8 , the flutter was of a rather unusual constant amplitude type and was different from that experienced during any other tests during this program. At $M = 7$, for example, at the data point small constant amplitude oscillations appeared in both the roll and pitch degrees of freedom. As the tunnel pressure was increased the amplitude of the oscillations increased but did not become divergent. When the model was retracted after hitting the pitch limit stops, the amplitude was approximately 10 times that of the constant amplitude flutter that was obtained initially. The roll-pitch amplitude ratio did

CONFIDENTIAL

not change as the flutter amplitude increased and the flutter frequency changed only 1% from the point the constant amplitude oscillations first appeared to the point at which the model was retracted. At $M = 8$ the flutter characteristics were similar to those obtained at $M = 7$, except that the amplitude growth was only a factor of two from the initiation of flutter to model retraction at the maximum P_o of the tunnel. Because of the peculiar nature of the flutter at $M = 7$ and 8 , additional tests were conducted at both of these Mach numbers and the results that were obtained substantiated the initial results.

Theoretical correlation of the experimental results was poor for this model configuration. The inclusion of structural damping in the analyses markedly improved the flutter frequency correlation, while it improved the correlation of the flutter velocity index to only a small extent. The decreasing trend in the Mach number range $6 < M < 7$ of the theoretical flutter velocity index in which the effects of structural damping have been included, is primarily due to the fact that the μ at $M = 7$ is more than twice the μ at $M = 6$. At $M = 8$ the μ is only 35% greater than at $M = 7$ and thus the theoretical flutter velocity index curve flattens out. This conclusion is supported by the theoretical results presented for μ equal to a constant which indicate that the flutter velocity index increases with increasing Mach number.

Figure 5 presents experimental and theoretical results obtained to show the effects of Mach number on the flutter characteristics of the $R = \frac{1}{2}$ wing having a frequency ratio of 0.544 . The variation of the flutter velocity index with Mach number is quite different from that which was obtained with the same model at a frequency ratio, $\omega_R/\omega_P = 0.514$. For example, for a frequency ratio, $\omega_R/\omega_P = 0.544$, divergent flutter was obtained at Mach numbers of 5, 6 and 7, while flutter could not be obtained at $M = 8$, within the tunnel limits as it was for a frequency ratio, $\omega_R/\omega_P = 0.514$. In addition, the drop in the flutter velocity index in the Mach number range $6 < M < 7$ was only 6% as compared to 28% for a frequency ratio, $\omega_R/\omega_P = 0.514$. At $M = 8$, for the model having a frequency ratio of $\omega_R/\omega_P = 0.544$, very little excitation from aerodynamic turbulence was experienced and, therefore, transient excitation was applied to the model. The transient excitation was obtained by injection of the model into the airstream. Excitation was initially applied at $V/b\omega_P\sqrt{\mu} = 1.50$ and then at every incremental increase in $V/b\omega_P\sqrt{\mu}$ of approximately 0.05. In every case, up to $V/b\omega_P\sqrt{\mu} = 1.85$, which corresponds to the upper limit of the tunnel, the transient motion provided by injection was quickly damped. The tests were repeated up to $V/b\omega_P\sqrt{\mu} = 1.80$ with the same results. The reason for this change in the flutter characteristics with frequency ratio at $M = 8$ could not be ascertained.

Correlation of the experimentally and theoretically determined flutter velocity indices is generally poor. It is noted that the theoretical analyses including structural damping resulted in poorer correlation of the flutter velocity

CONFIDENTIAL

index but a much better prediction of the flutter frequency. The reason for the "S" shape of the theoretical curve of the flutter velocity index based on analyses using piston theory and in which the effects of structural damping have been included is believed to be due to the fact that the increase in μ from $M = 6$ to $M = 7$ is approximately 10 times larger than the increase from $M = 7$ to $M = 8$.

Figure 6 presents the theoretical and experimental results obtained with the $R = \frac{1}{2}$ model at a frequency ratio, $\omega_r/\omega_p = 0.670$. The results obtained at this frequency ratio are very similar to the results obtained with the model at a frequency ratio, $\omega_r/\omega_p = 0.544$, except that divergent flutter was obtained at $M = 8$ with $\omega_r/\omega_p = 0.670$. At $M = 8$ the model changed from a stable condition to a rapidly divergent unstable condition with a very small change in the flutter velocity index. Again, the reason for this change in the flutter characteristics at $M = 8$ with a change in the frequency ratio is not known. It is noted, as with the results obtained at the other frequency ratios, that the inclusion of structural damping in the theoretical analyses was destabilizing and also resulted in much better prediction of the flutter frequency.

Figure 7 presents a comparison of the theoretical and experimental flutter velocity indices vs Mach number for the $R = \frac{1}{2}$ model for the three different frequency ratios. The important thing to be noted is that for each frequency ratio there is an unconservative trend in the Mach number range of $6 < M < 7$, and then a conservative trend apparent at $M = 8$.

B. FLUTTER RESULTS OBTAINED WITH THE BLUNT NOSE, $R = 1$ MODEL

1. Effect of Frequency Ratio Variation

Figure 8 shows the experimental results that were obtained at $M = 6$ to describe the effects of frequency ratio on the flutter velocity index for an $R = 1.0$ model having a semicircular leading edge whose radius is equal to $c/2$. Also shown, for purposes of comparison, are the experimental results previously reported in Ref. 1 obtained with a model having the same nondimensional flutter parameters but having the basic modified double wedge profile. The flutter results obtained for this model at a frequency ratio, $\omega_r/\omega_p = 0.50$ indicates the leading edge bluntness is stabilizing which is in agreement with experimental results reported in Ref. 3 and with theoretical results reported in Ref. 5.

Comparison of the results presented in Fig. 8 for the blunt and the bevelled edge models at $M = 6$ indicates that for frequency ratios, $\omega_r/\omega_p < 0.65$, the effect of leading-edge bluntness is stabilizing. Comparison of the curves indicates, however, that above this frequency ratio, the stabilizing effect of

CONFIDENTIAL

leading edge bluntness rapidly diminishes. Thus, for all-movable control surfaces, whose bending to pitch frequency ratio may be approximately unity, the stabilizing effect of leading edge bluntness may be nonexistent.

2. Effects of Mach Number Variation on $R = 1$, Blunt Nose Model

Figure 9 presents the experimental results that were obtained to determine the effects of Mach number on the flutter characteristics of the blunt nose model. As indicated, results were obtained throughout the Mach number range of $5 < M < 8$ for the blunt nose model having a frequency ratio, $\omega_R/\omega_p = 0.847$. Although flutter was obtained at $M = 6$ for the blunt nose model having a frequency ratio, $\omega_R/\omega_p = 0.679$, flutter could not be obtained at $M = 7$ within the limits of the tunnel. The data presented in Fig. 8 shows that for $\omega_R/\omega_p = 0.679$, if the curve describing the variation of the flutter velocity index with frequency ratio shifted slightly to higher frequency ratios at $M = 7$, flutter would probably not be obtained for the model having this frequency ratio. This is believed to be the reason why flutter was obtained at $M = 6$ and not at $M = 7$ for this model configuration.

The results obtained with the blunt nose model, the $R = \frac{1}{2}$ modified double wedge model and with the $R = 1$ modified double wedge models having center-of-gravity positions at both the 45% and 50% chord positions (Ref. 1) are interesting in that the destabilizing trend in the Mach number range of $6 < M < 7$ was obtained with all of these configurations. It might be concluded, therefore, that for models having a thickness ratio of 4%, the destabilizing trend in the Mach number range $6 < M < 7$ does not appear to be significantly dependent upon the profile, center-of-gravity position or the aspect ratio.

C. FLUTTER RESULTS OBTAINED WITH THE 8% THICK MODEL

In Figs. 10 and 11, experimental and theoretical results are presented for the 8% thick model as well as data for the 4 and 6% thick models taken from Ref. 1. The experimental results indicate that at Mach numbers of 5 and 6 there is about a 15% decrease in the flutter velocity index for an increase in thickness from 4% to 6%. An increase in thickness from 6% to 8% results in a 5% decrease in the flutter velocity index.

Comparison of experimental results with theoretical results based on piston theory aerodynamics both neglecting and including the effects of structural damping shows that piston theory, while adequately predicting the flutter velocity index at thickness ratios of 4% and 6% at $M = 5$ and 6, tends to a more conservative prediction as thickness increases above 6%. It is further noted that the inclusion of structural damping in the analyses results in good correlation with the experimental frequency while correlation is poor when structural damping is neglected.

WADD TR 60-328, Suppl. 1

CONFIDENTIAL

Figure 12 shows the variation of the flutter frequency and velocity index with Mach number for $R = 1$ models of 4%, 6% and 8% thickness ratios. While the 4% thick model shows a destabilizing trend as Mach number is increased from 6 to 7, the 6% model shows the opposite trend. No conclusion can be drawn as to the variation of the flutter velocity index with Mach number above $M = 6$, for the 8% model since data was not obtained for $M > 6$ due to damage suffered by the model during violent flutter at a lower Mach number.

WADD TR 60-328, Suppl. 1

CONFIDENTIAL

CONFIDENTIAL

VII. CONCLUSION AND RECOMMENDATIONS

It is believed that the general objective of this supplementary flutter program was accomplished. On the basis of the experimental tests and the theoretical analyses conducted, the following specific conclusions may be drawn:

1. Over the frequency ratio range tested at $M \approx 6$ the basic $R = \frac{1}{2}$ model appears to be slightly more stable than the basic $R = 1$ model.
2. The effect of blunting the leading edge of the basic modified double wedge profile model at $M \approx 6$ is stabilizing over the frequency ratio range covered.
3. The effects of increasing thickness were found to be destabilizing at $M = 5$ and 6 . Piston theory predictions of the effects of thickness were found to be conservative at a thickness ratio of 8% whereas they very closely predicted the flutter velocity index at thickness ratios of 4 and 6% .
4. The variations of the flutter velocity index with Mach number for the $R = \frac{1}{2}$ model and for the $R = 1$ blunt nose model appeared to be dependent on the frequency ratio. For all the frequency ratios tested, there is a destabilizing trend in the range $6 < M < 7$, and the start of a stabilizing trend apparent at $M = 8$. The amount of destabilization between $M = 6$ and 7 and the amount of stabilization at $M = 8$ appear to be dependent on frequency ratio although additional data would be desirable to better define this effect of frequency ratio. Piston theory does not adequately predict these variations.
5. The predicted values of flutter frequency using piston theory were generally greater than the experimental values when structural damping was not included in the analyses, but the correlation was generally improved when structural damping was included.

The results presented in the main body of this report (Ref. 1) as well as those presented in this supplement strongly support the recommendation that a theoretical research program be undertaken in an attempt to explain the unusual hypersonic characteristics that have been reported.

In addition it is recommended that the following experimental research work be undertaken.

1. Additional experimental investigations should be undertaken to define more clearly the parameters which cause the unpredicted flutter trend with increasing Mach number above 6 . The investigations should also obtain data to determine if the unpredicted trend continues to higher Mach numbers.

WADD TR 60-328, Suppl. 1

CONFIDENTIAL

2. Tests should be conducted to obtain more data for $R = \frac{1}{2}$ and $R = 1$ model configurations. The primary purpose of such tests should be to obtain flutter data to define the effects caused by larger variations of the parameters already tested.

3. Tests should be conducted to obtain experimental data that can be used to check piston theory predictions of the effects of taper ratio, sweep, aspect ratio and of profiles other than those already tested.

UNCLASSIFIED

VIII. REFERENCES

1. White, R. P. Jr., King, S. R. and Balcerak, J. C., Flutter Model Tests at Hypersonic Speeds M = 5 to 7, (UNCLASSIFIED Title), WADD TR 60-328, May 1960 (CONFIDENTIAL Report).
2. Chawla, J. P., "Aeroelastic Instability at High Mach Number", Journal of Aeronautical Sciences, Vol. 25, No. 4, April 1958.
3. Martucelli, J. R., Flutter Model Tests at Mach Numbers 1.5 - 5.0 (UNCLASSIFIED Title), WADD TR 59-407, September 1959 (CONFIDENTIAL Report).
4. McLellan, C. H., Bertram, M. H. and Moore, J. A., An Investigation of Four Wings of Square Plan Form at a Mach Number of 6.9 in the Langley 11 - Inch Hypersonic Tunnel, NACA Technical Rept. 1310, 1957.
5. Morgan, H. G., Runyan, H. H. and Huckel, V. "Theoretical Considerations of Flutter at High Mach Numbers", Journal of Aeronautical Sciences, Vol. 25, No. 6, June 1958.

WADD TR 60-328, Suppl. 1

UNCLASSIFIED

TABLE I. SUMMARY OF NONDIMENSIONAL MODEL PARAMETERS

Model Designation / Model Parameters	τ/c	r_p^2	w_R/w_P	C.G. % CHORD	P.A. % CHORD	R	Profile
SR-19-1	0.04	0.314	0.496	49.8	40.0	1	Basic
SR-20-9	0.04	0.303	0.492	49.9	40.0	$\frac{1}{2}$	Basic
SR-21-9	0.04	0.303	0.493	49.9	40.0	$\frac{1}{2}$	Basic
SR-22-9	0.04	0.303	0.514	49.9	40.0	$\frac{1}{2}$	Basic
SR-23-9	0.04	0.303	0.544	49.9	40.0	$\frac{1}{2}$	Basic
SR-24-9	0.04	0.303	0.570	49.9	40.0	$\frac{1}{2}$	Basic
SR-25-9	0.04	0.303	0.670	49.9	40.0	$\frac{1}{2}$	Basic
SR-26-7	0.04	0.314	0.489	50.0	40.0	1	Blunt Nose*
SR-27-7	0.04	0.314	0.502	50.0	40.0	1	"
SR-28-7	0.04	0.314	0.628	50.0	40.0	1	"
SR-29-7	0.04	0.314	0.656	50.0	40.0	1	"
SR-30-7	0.04	0.314	0.670	50.0	40.0	1	"
SR-31-7	0.04	0.314	0.679	50.0	40.0	1	"
SR-32-7	0.04	0.314	0.693	50.0	40.0	1	"
SR-33-7	0.04	0.314	0.761	50.0	40.0	1	"
SR-34-7	0.04	0.314	0.847	50.0	40.0	1	"
SR-35-8	0.08	0.299	0.489	50.0	40.0	1	Basic

* The blunt nose model has a semicircular leading edge of radius $\tau/2$

UNCLASSIFIED

TABLE II. PITCH INERTIA OF SUSPENSION SYSTEM
FOR SEMIRIGID MODEL CONFIGURATIONS

MODEL CONFIGURATION	SUSPENSION PITCH INERTIA X 10^3 lb.-in.-sec ²
SR-19-1	0.831
SR-20-9	0.512
SR-21-9	0.512
SR-22-9	0.512
SR-23-9	0.512
SR-24-9	0.512
SR-25-9	0.512
SR-26-7	0.547
SR-27-7	0.547
SR-28-7	0.547
SR-29-7	0.547
SR-30-7	0.547
SR-31-7	0.547
SR-32-7	0.547
SR-33-7	0.547
SR-34-7	0.547
SR-35-8	0.512

WADD TR 60-328, Suppl. 1

UNCLASSIFIED

TABLE III. MASS PROPERTIES OF SEMIRIGID MODELS

MODEL NO.	TOTAL MASS $\times 10^4$ Lb.-Sec.^2 In.	C. G. % CHORD	TOTAL ROLL INERTIA $\times 10^3$ Lb. In.-Sec.^2	TOTAL PITCH INERTIA $\times 10^3$ Lb.-In.-Sec^2
1	7.84	48.5	9.08	1.313
7	8.38	48.5	8.87	1.543
8	9.38	49.0	10.31	1.801
9	5.08	48.3	1.40	0.758

WADD TR 60-328, Suppl. 1

UNCLASSIFIED

TABLE IV. SUMMARY OF ZERO AIRSPEED VIBRATION
TEST RESULTS, SEMIRIGID MODELS

MODEL CONFIGURATION	UNCOUPLED ROLL CPS	UNCOUPLED PITCH CPS	ω_R/ω_P	1st COUPLED MODE CPS	2nd COUPLED MODE CPS
SR-19-1	27.0	54.5	0.496	26.9	58.1
SR-20-9	28.2	57.3	0.492	27.9	62.7
SR-21-9	26.8	54.4	0.493	26.4	58.5
SR-22-9	27.3	53.0	0.514	27.0	57.4
SR-23-9	27.2	50.0	0.544	26.8	54.9
SR-24-9	27.3	47.9	0.570	26.9	52.0
SR-25-9	33.5	50.0	0.670	32.6	55.5
SR-26-7	21.4	43.8	0.489	21.2	47.1
SR-27-7	23.3	46.4	0.502	23.1	49.5
SR-28-7	22.3	35.5	0.628	21.8	38.8
SR-29-7	23.3	35.5	0.656	22.7	38.8
SR-30-7	23.8	35.5	0.670	23.2	39.6
SR-31-7	24.1	35.5	0.679	23.5	39.6
SR-32-7	24.6	35.5	0.693	23.9	40.0
SR-33-7	27.0	35.5	0.761	26.0	40.5
SR-34-7	40.3	47.6	0.847	38.5	55.4
SR-35-8	38.6	78.9	0.489	38.1	85.0

WADD TR 60-328, Suppl. 1

CONFIDENTIAL

TABLE V. SUMMARY OF WIND TUNNEL TEST RESULTS

MODEL CONFIGURATION	P ₀ PSIA	T ₀ OR	MACH NO.	$\rho \times 10^8$ LB-SEC ² /IN ⁴	V FT./SEC.	μ	$\frac{V}{b\omega_p\sqrt{\mu}}$	$\frac{\omega_F}{CPS}$	$\frac{\omega_F}{\omega_p}$
SR-19-1	410	896	6.03	0.940	3076	372	1.863	36.3	0.666
SR-20-9	615	930	6.04	1.365	3131	315	1.960	36.6	0.639
SR-21-9(1)	561	897	6.02	1.296	3077	332	1.975	36.0	0.662
SR-22-9	445	922	6.03	0.992	3120	434	1.797	32.6	0.615
SR-22-9	497	1143	6.96	0.471	3526	913	1.400	30.5	0.574
SR-22-9	874	1399	8.04	0.349	4026	1234	1.376	29.7	0.560
SR-23-9	163	687	5.00	1.089	2623	395	1.680	34.0	0.680
SR-23-9	398	893	6.02	0.923	3070	466	1.811	33.8	0.676
SR-23-9	676	1164	7.00	0.613	3562	702	1.712	31.5	0.630
SR-23-9*(2)(5)	1421	1320	8.11	0.578	3839	744	1.792	-	-
SR-23-9*(2)	1550	1391	8.11	0.598	3940	719	1.871	-	-
SR-24-9	299	921	5.00	0.682	3116	631	1.849	33.0	0.689
SR-25-9	106	672	5.00	0.724	2594	595	1.354	38.6	0.772
SR-25-9	235	872	5.98	0.575	3032	749	1.410	37.3	0.746
SR-25-9	414	1083	6.96	0.414	3434	1038	1.357	36.6	0.732
SR-25-9(3)	815	1385	8.04	0.329	3930	1309	1.383	37.8	0.756
SR-26-7	440	899	6.03	1.008	3081	339	2.432	-	-
SR-27-7	311	923	6.00	0.709	3119	482	1.949	-	-
SR-28-7	388	910	6.02	0.882	3098	387	2.825	-	-
SR-29-7	430	888	6.03	0.997	3062	343	2.966	-	-
SR-30-7	436	900	6.03	0.995	3083	344	2.979	-	-
SR-31-7	144	884	5.95	0.355	3049	962	1.763	27.0	0.761
SR-31-7*(6)	666	1061	7.01	0.658	3398	519	2.674	-	-
SR-32-7	215	957	5.97	0.484	3176	707	2.142	28.0	0.789
SR-33-7	106	863	5.94	0.270	3010	1266	1.517	29.8	0.839
SR-34-7	45	704	4.95	0.304	2648	1126	1.056	41.7	0.876
SR-34-7	166	868	5.96	0.413	3020	827	1.404	41.8	0.878
SR-34-7	235	1119	6.98	0.225	3490	1522	1.196	41.0	0.861
SR-34-7(4)(5)	498	1269	7.95	0.231	3758	1480	1.306	40.4	0.849
SR-34-7(4)	599	1309	8.02	0.259	3820	1320	1.406	40.4	0.849
SR-35-8(1)	271	714	5.02	1.713	2676	232	1.417	51.2	0.849
SR-35-8(5)	583	864	6.05	1.368	3022	290	1.432	50.0	0.634

*Configurations for which flutter was not obtained:

- (1) T₀ obtained from tunnel strip chart
- (2) P₀ vs. Mach No. calibration not available for these pressures. Mach No. assumed to be the same as that at highest P₀ for which calibration is available.
- (3) P₀ obtained visually from pressure gauge at flutter. T₀ obtained from tunnel strip chart.
- (4) Model excited by injection while P₀ was held constant. At lower point model took 16 seconds to decay to 0.12 of initial amplitude caused by excitation. Upper point is the constant amplitude flutter point; amplitude is 1.19 times that of initial amplitude of lower point.
- (5) Data obtained below liquefaction temperature.

CONFIDENTIAL

UNCLASSIFIED

TABLE VI. SUMMARY OF CALCULATED FLUTTER RESULTS

MODEL CONFIGURATION	MACH NO.	CALCULATION EXCLUDING STRUCTURAL DAMPING		CALCULATIONS INCLUDING STRUCTURAL DAMPING**	
		$V/b\omega_p\sqrt{\mu}$	ω_F/ω_p	$V/b\omega_p\sqrt{\mu}$	ω_F/ω_p
SR-20-9	6.04	1.767	0.777	1.743	0.638
SR-22-9	6.04	1.720	0.785	1.660	0.644
SR-22-9	6.96	1.749	0.777	1.628	0.618
SR-22-9	8.04	1.777	0.769	1.628	0.601
SR-23-9	5.00	1.610	0.804	1.549	0.682
SR-23-9	6.02	1.653	0.795	1.575	0.665
SR-23-9	7.00	1.685	0.787	1.572	0.647
SR-23-9*	8.11	1.716	0.780	1.595	0.639
SR-24-9	6.00	1.609	0.804	1.489	0.678
SR-25-9	5.00	1.323	0.851	1.201	0.751
SR-25-9	5.98	1.375	0.843	1.253	0.748
SR-25-9	6.96	1.417	0.836	1.283	0.742
SR-25-9	8.04	1.454	0.829	1.311	0.734
SR-35-8	5.00	1.311	0.746	1.323	0.643
SR-35-8	6.05	1.330	0.735	1.328	0.625

* Configuration for which flutter was not obtained

** For Model No. 8 $g_R = 0.008$ & $g_p = 0.03$

For Model No. 9 $g_R = 0.015$ & $g_p = 0.04$

WADD TR 60-328, Suppl. 1

CONFIDENTIAL

TABLE VII. COMPARISON OF CALCULATED & EXPERIMENTAL FLUTTER RESULTS

MODEL CONFIGURATION	MACH NUMBER	CALCULATIONS EXCLUDING DAMPING		CALCULATIONS INCLUDING DAMPING**	
		$\frac{[V/b\omega_p\sqrt{\mu}]_{EXP}}{[V/b\omega_p\sqrt{\mu}]_{CALC}}$	$\frac{\omega_{F EXP}}{\omega_{F CALC}}$	$\frac{[V/b\omega_p\sqrt{\mu}]_{EXP}}{[V/b\omega_p\sqrt{\mu}]_{CALC}}$	$\frac{\omega_{F EXP}}{\omega_{F CALC}}$
SR-20-9	6.04	1.109	0.822	1.124	1.002
SR-22-9	6.04	1.045	0.783	1.082	0.955
SR-22-9	6.96	0.800	0.739	0.860	0.929
SR-22-9	8.04	0.774	0.728	0.845	0.932
SR-23-9	5.00	1.043	0.846	1.084	0.997
SR-23-9	6.02	1.096	0.850	1.150	1.016
SR-23-9	7.00	1.016	0.800	1.089	0.974
SR-23-9*	8.11	1.090	-	1.173	-
SR-24-9	6.00	1.025	0.857	1.107	1.016
SR-25-9	5.00	1.023	0.907	1.127	1.028
SR-25-9	5.98	1.025	0.885	1.125	0.997
SR-25-9	6.96	0.958	0.876	1.058	0.986
SR-25-9	8.04	0.951	0.912	1.055	1.030
SR-35-8	5.00	1.081	0.870	1.071	1.009
SR-35-8	6.05	1.077	0.862	1.078	1.014

* Configuration for which flutter was not obtained

** For Model No. 8 $g_R = 0.008$ & $g_P = 0.03$

For Model No. 9 $g_R = 0.015$ & $g_P = 0.04$

WADD TR 60-328, Suppl. 1

UNCLASSIFIED

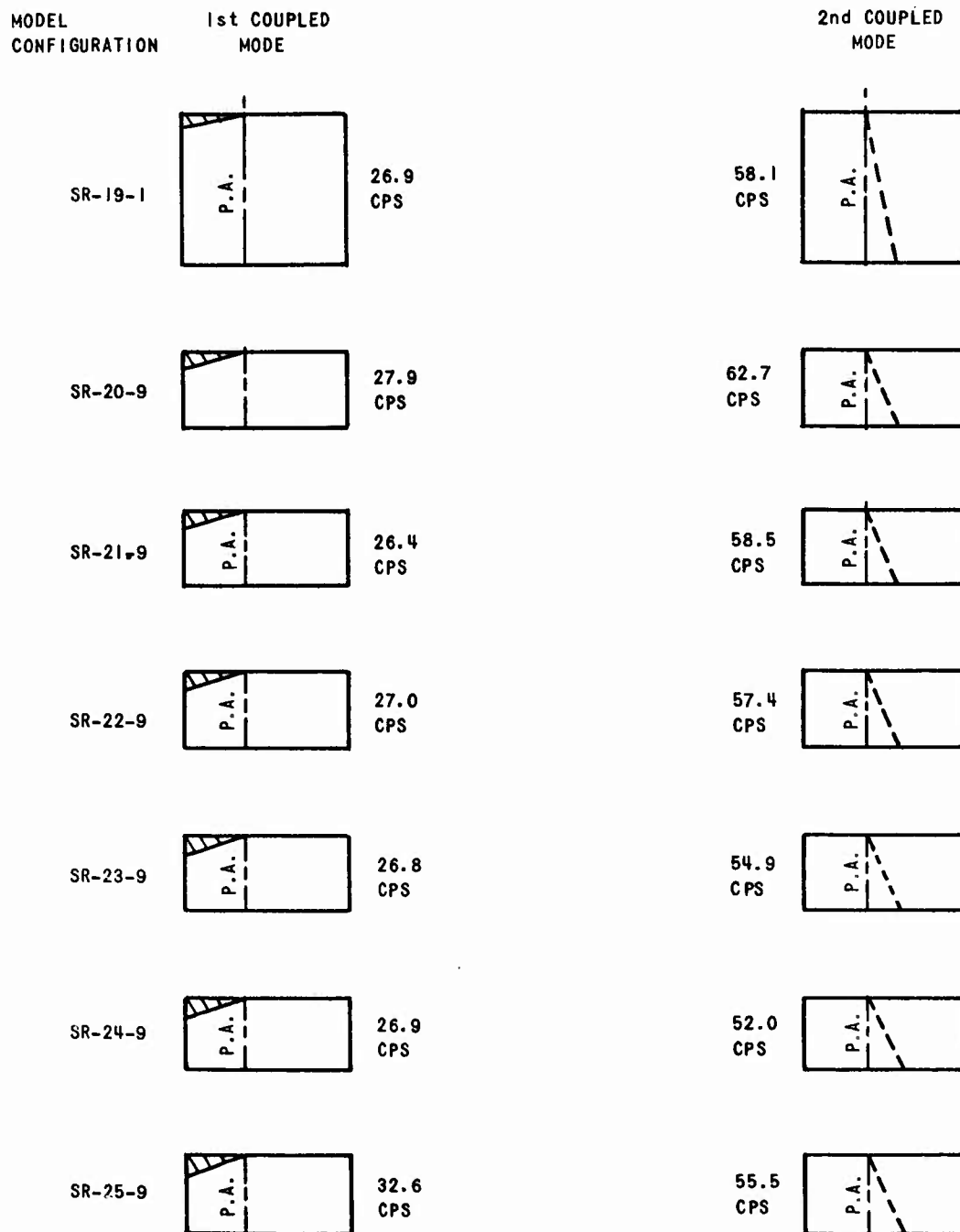


FIGURE 1 MEASURED COUPLED MODE MODE LINES AND FREQUENCIES, SEMIRIGID MODELS

UNCLASSIFIED

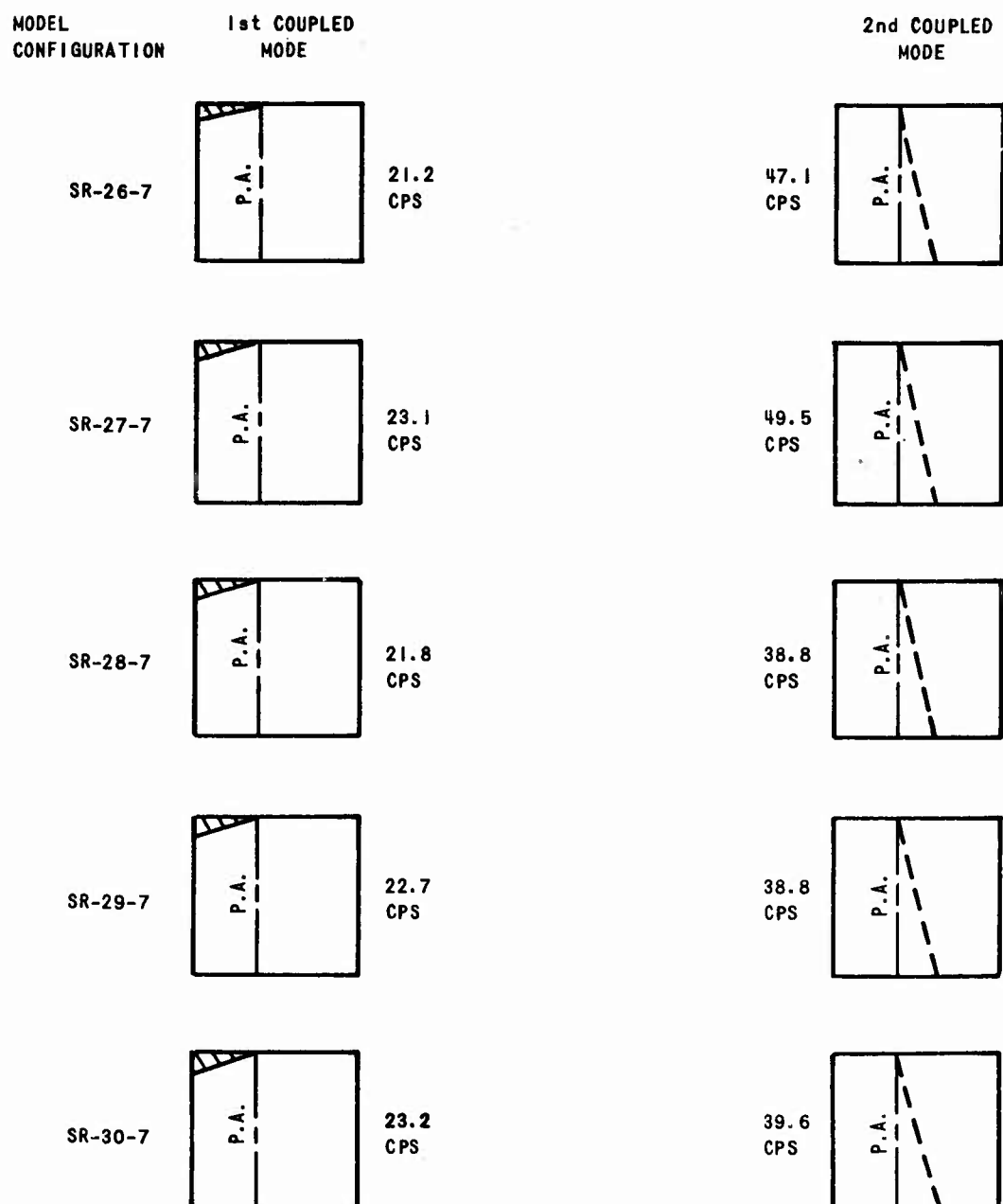


FIGURE 1 MEASURED COUPLED MODE NODE LINES AND FREQUENCIES -
SEMIRIGID MODELS (CONT'D)

UNCLASSIFIED

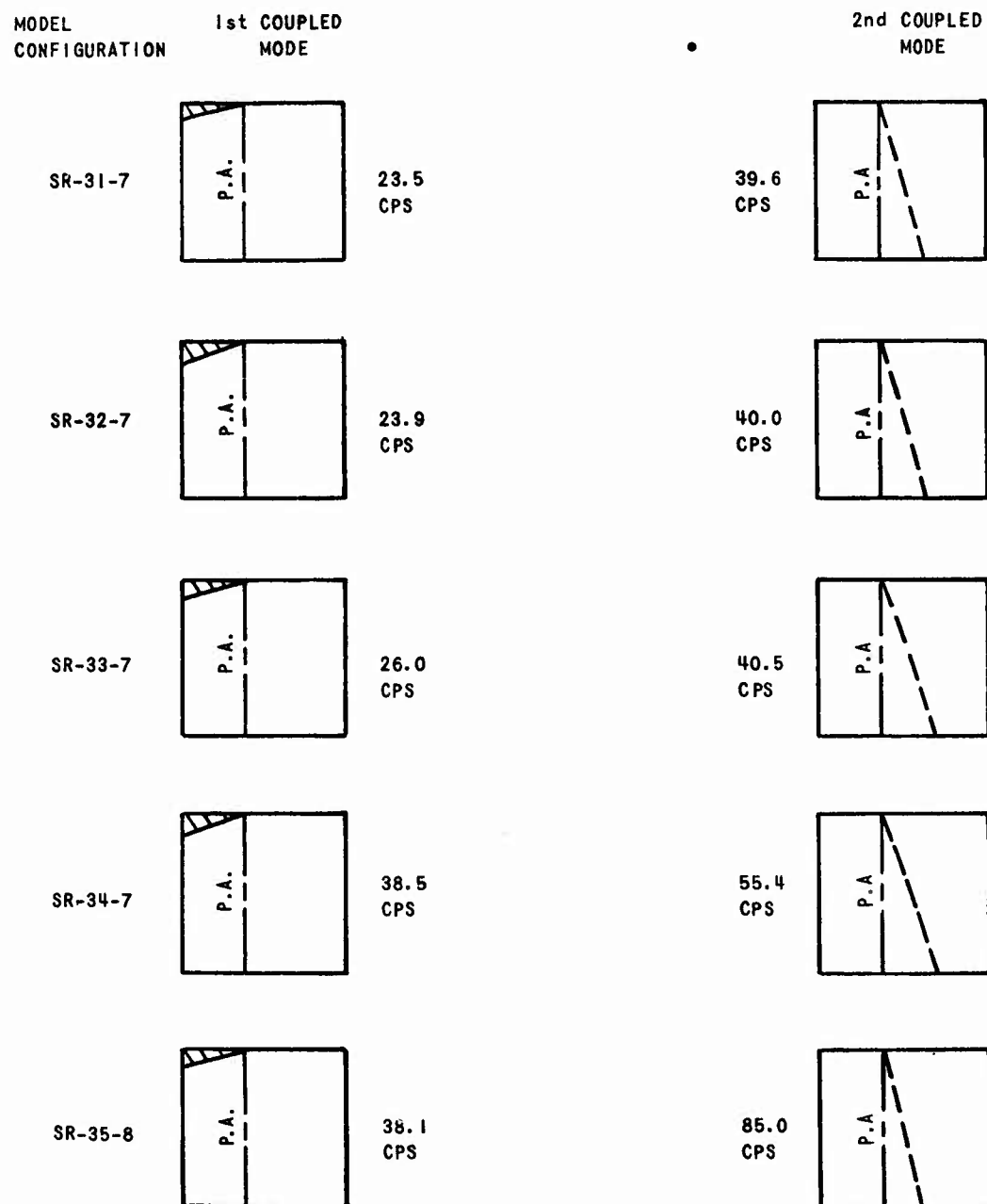


FIGURE 1 MEASURED COUPLED MODE NODE LINES AND FREQUENCIES -
SEMIRIGID MODELS (CONCLUDED)

WADD TR 60-328, Suppl. 1

22

UNCLASSIFIED

UNCLASSIFIED

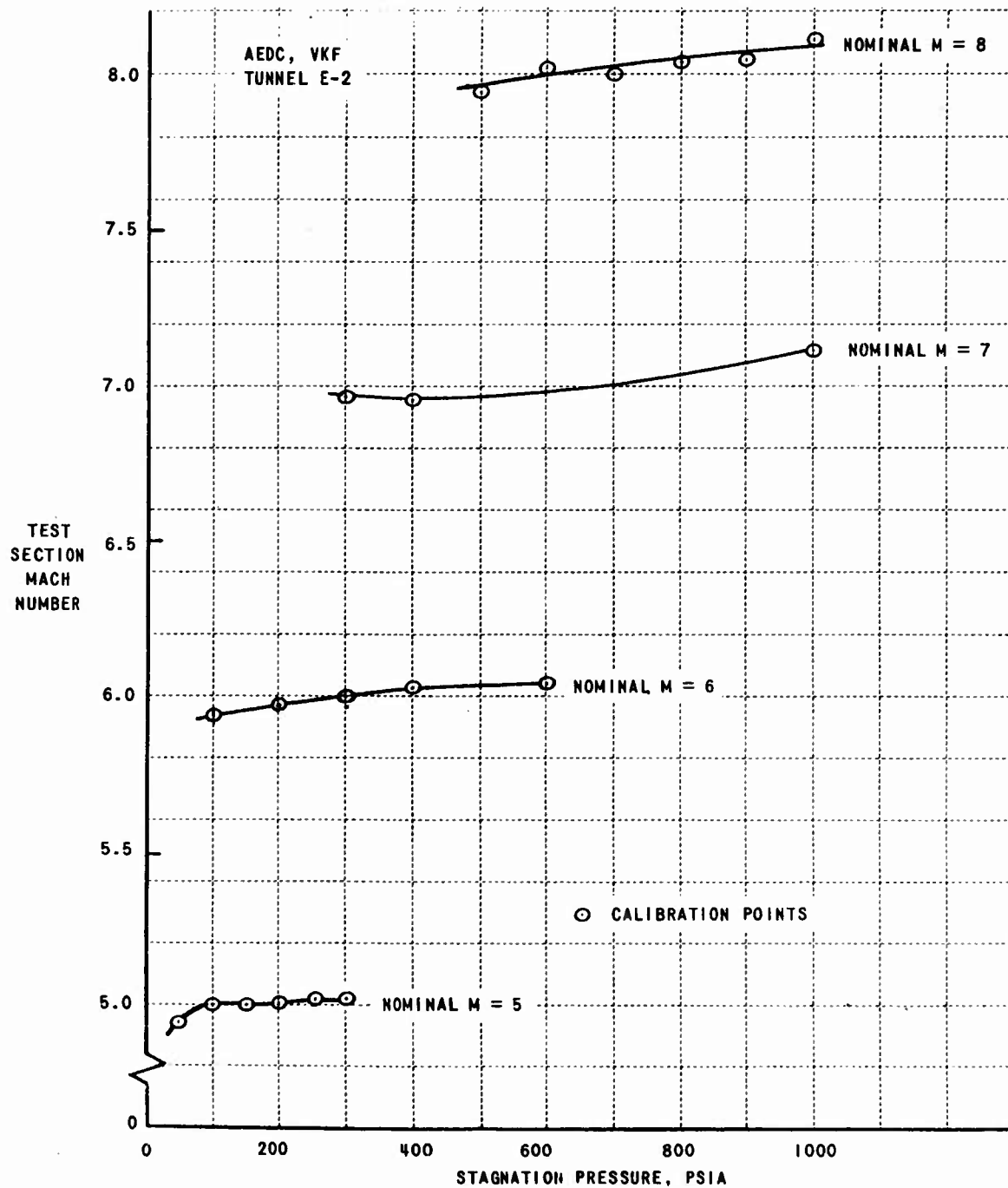


Figure 2 TEST SECTION MACH NUMBER VS. STAGNATION PRESSURE

UNCLASSIFIED

CONFIDENTIAL

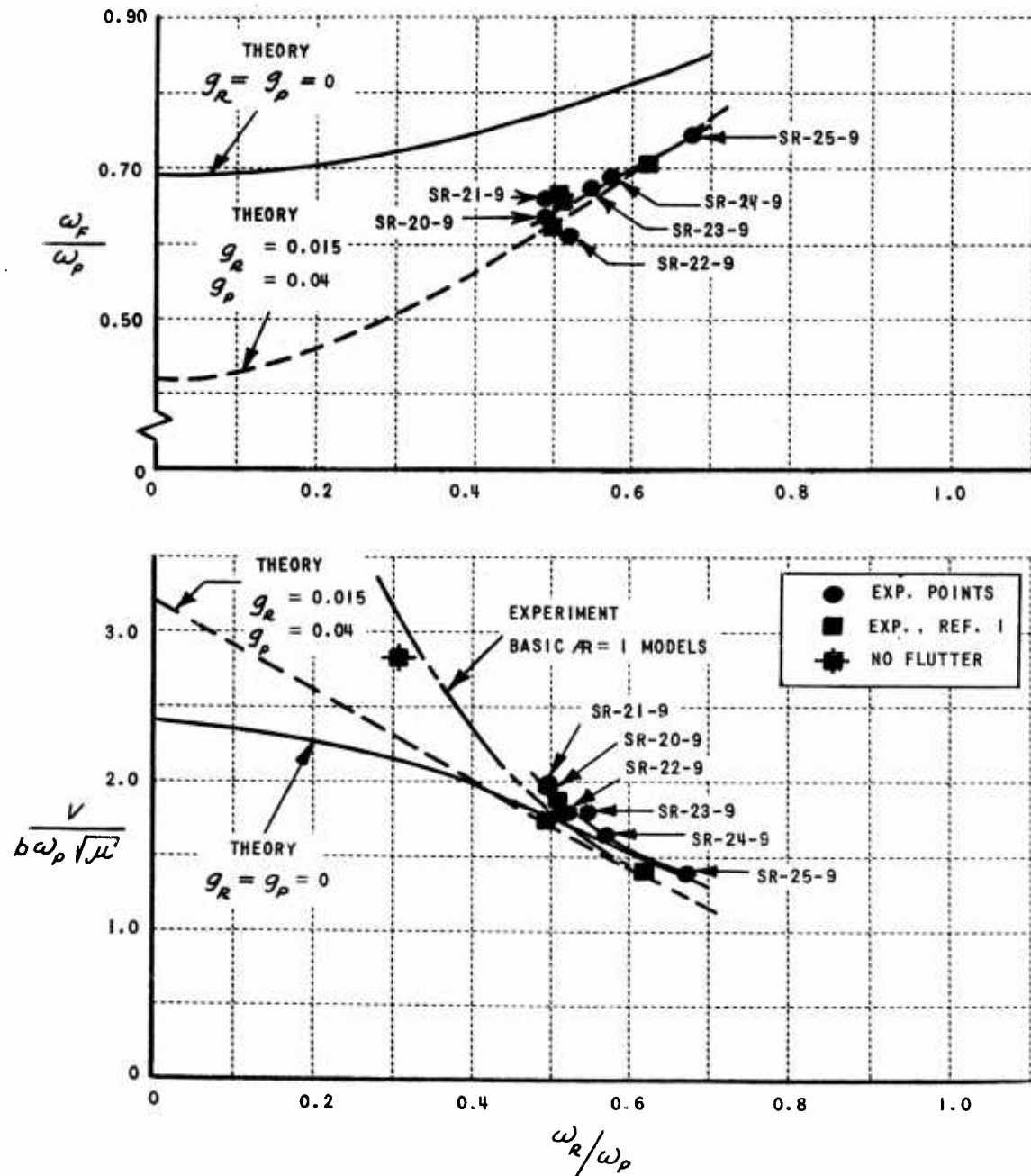


FIGURE 3 $\frac{\omega_F}{\omega_p}$ & $V/b\omega_p\sqrt{\mu}$ VS. ω_R/ω_p , $R = 1/2$ MODEL, MACH NO. ≈ 6.0

CONFIDENTIAL

CONFIDENTIAL

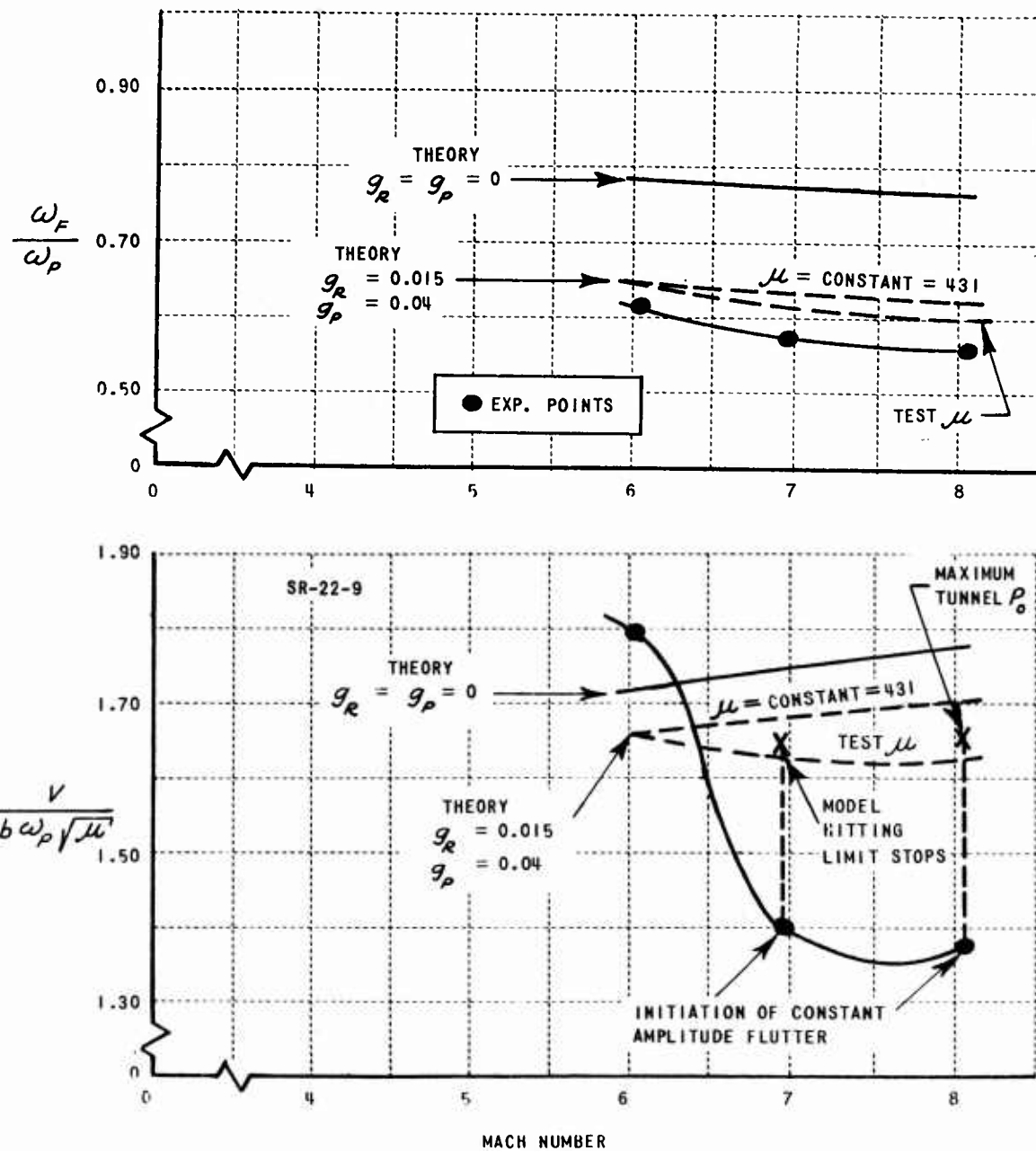


FIGURE 4 ω_F/ω_p & $V/b\omega_p\sqrt{\mu}$ VS. MACH NO., $R = 1/2$ MODEL, $\omega_R/\omega_p = 0.514$

CONFIDENTIAL

CONFIDENTIAL

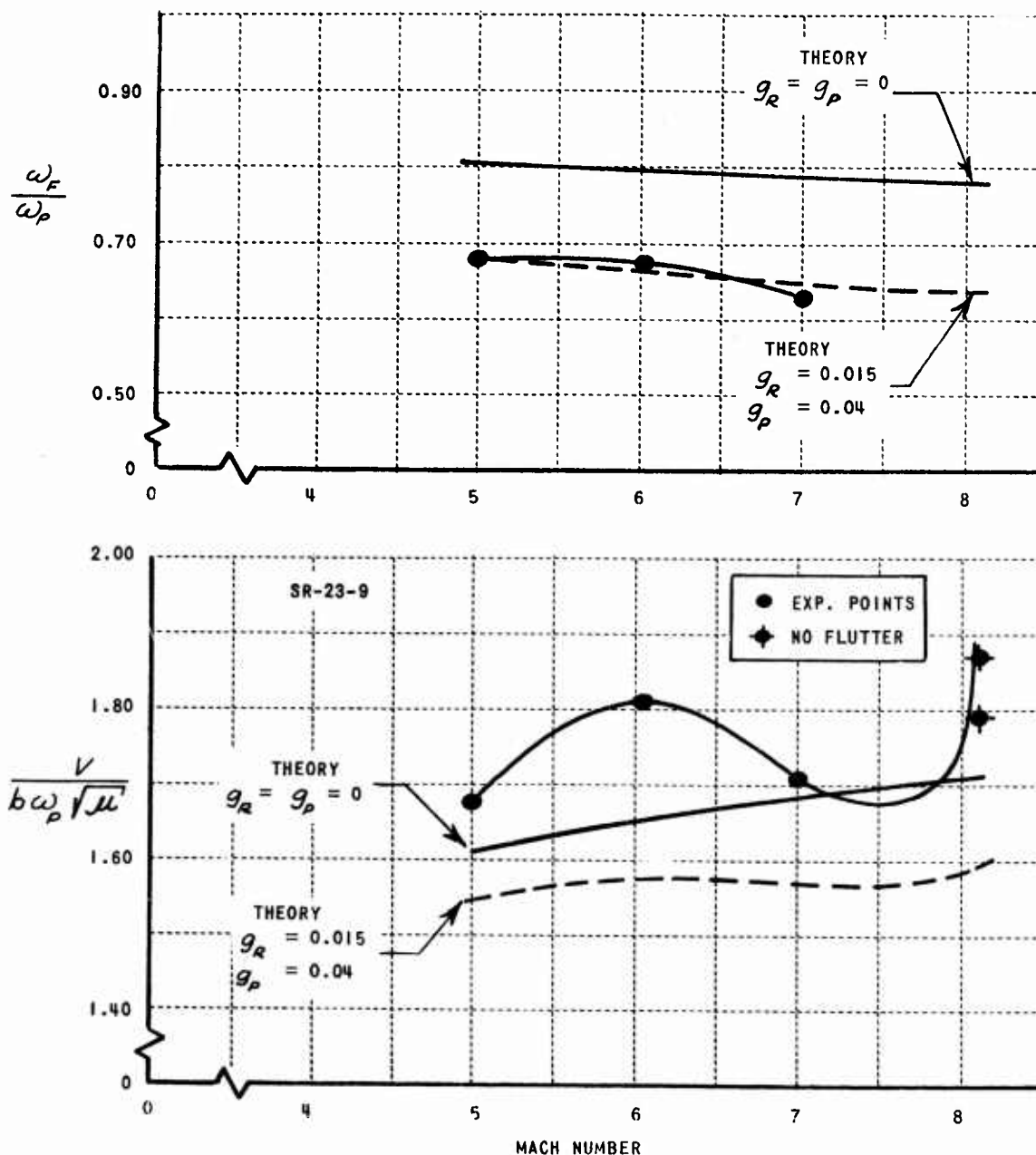


FIGURE 5 ω_F/ω_p & $V/b\omega_p\sqrt{\mu}$ VS. MACH NO., $AR = 1/2$ MODEL,
 $\omega_R/\omega_p = 0.544$

CONFIDENTIAL

CONFIDENTIAL

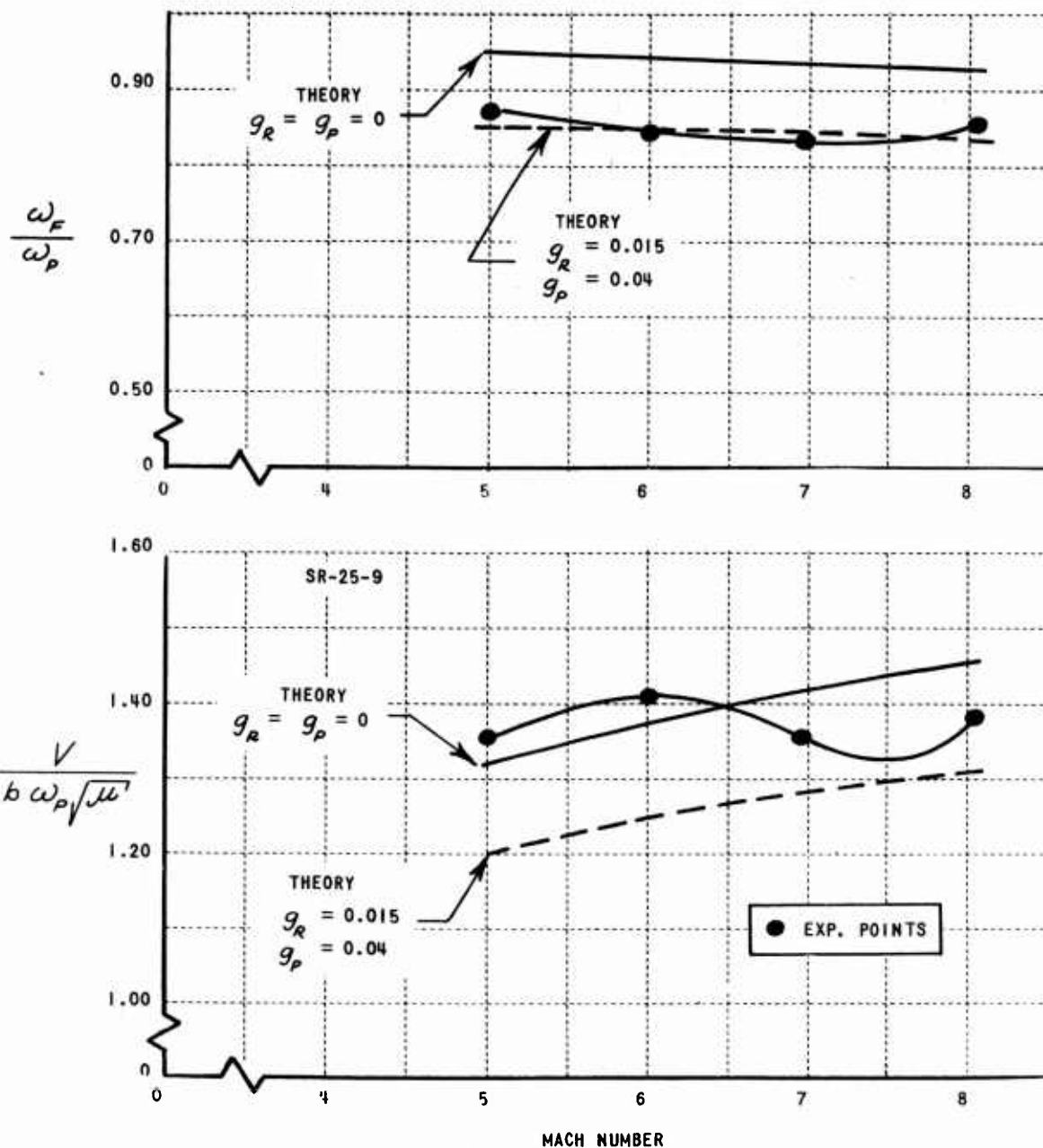


FIGURE 6 $\frac{\omega_F}{\omega_p} \neq \frac{V}{b \omega_p \sqrt{\mu'}}$ VS. MACH NO., $AR = 1/2$ MODEL,
 $\frac{\omega_R}{\omega_p} = 0.670$

CONFIDENTIAL

CONFIDENTIAL

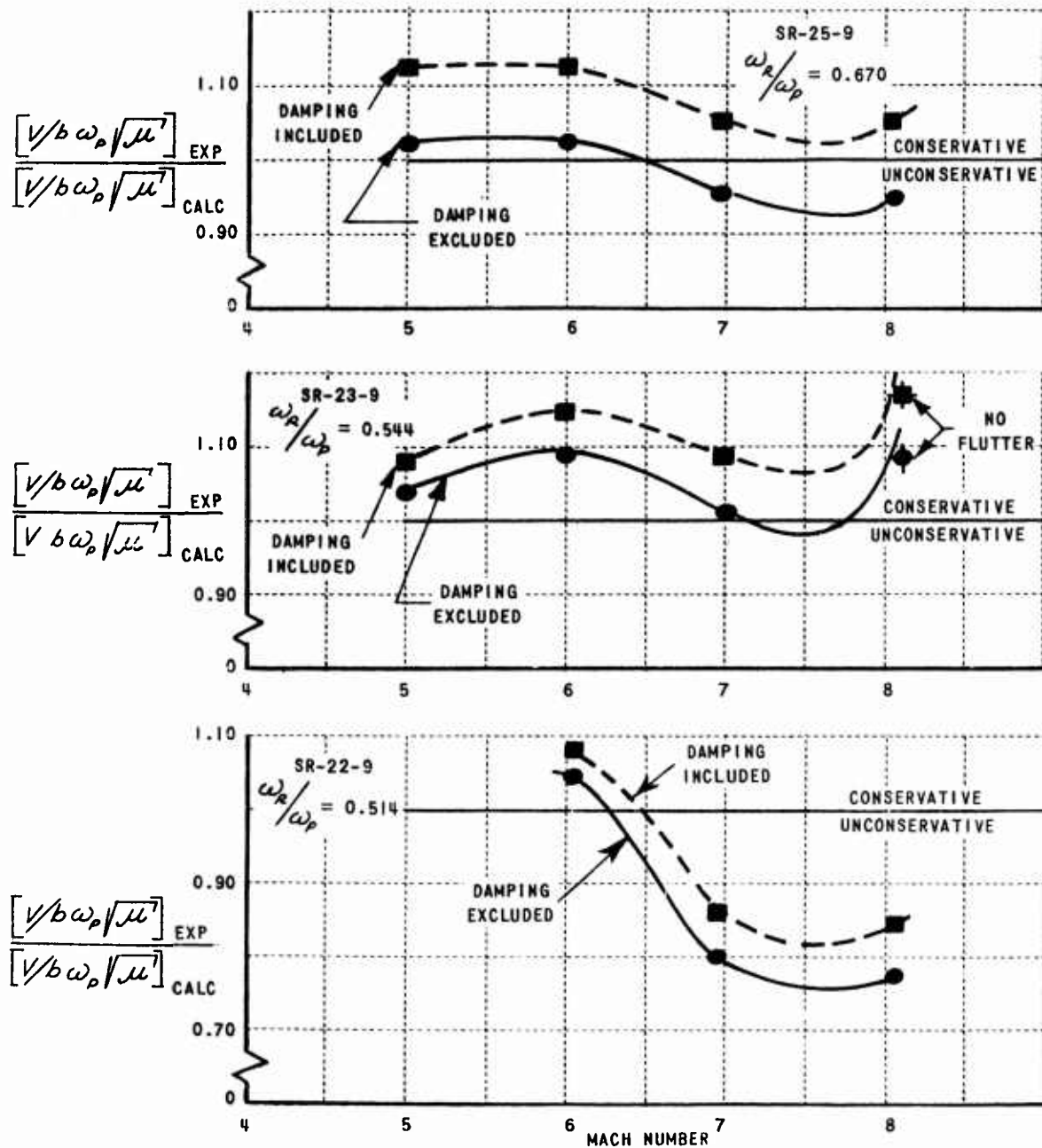


Figure 7 $\frac{[V/b\omega_p\sqrt{\mu'}]_{EXP}}{[V/b\omega_p\sqrt{\mu'}]_{CALC}}$ VS. MACH NUMBER
FOR VARIOUS FREQUENCY RATIOS, $R = 1/2$ MODEL

CONFIDENTIAL

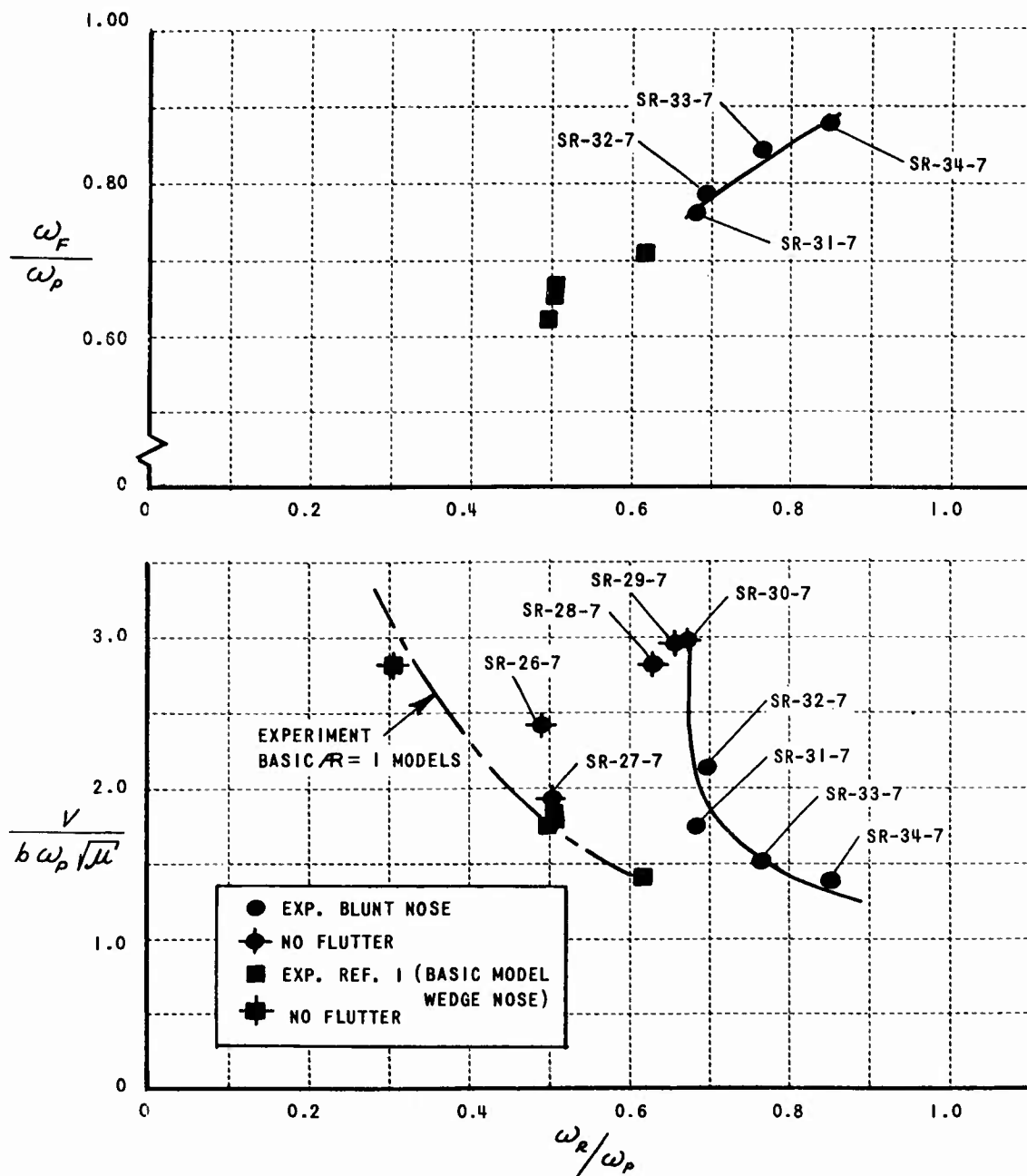


FIGURE 8 ω_F/ω_p & $V/b\omega_p\sqrt{\mu}$ vs. ω_r/ω_p BLUNT NOSE MODEL,
MACH NO. $\cong 6.0$

CONFIDENTIAL

CONFIDENTIAL

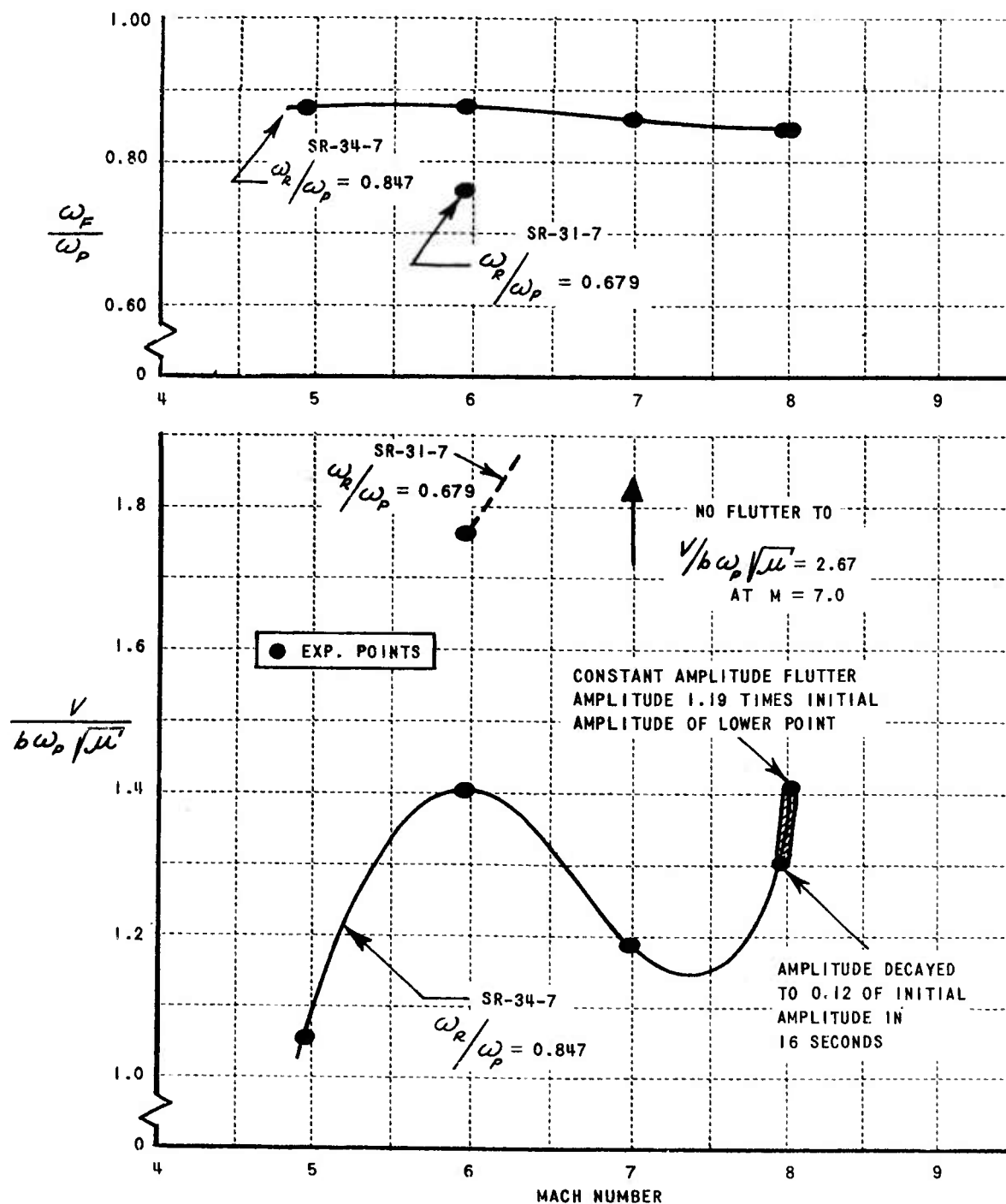


Figure 9 $\frac{\omega_F}{\omega_P}$ & $\frac{V}{b\omega_P\sqrt{\mu}}$ VS. MACH NUMBER FOR VARIOUS FREQUENCY RATIOS, BLUNT NOSE MODEL

CONFIDENTIAL

CONFIDENTIAL

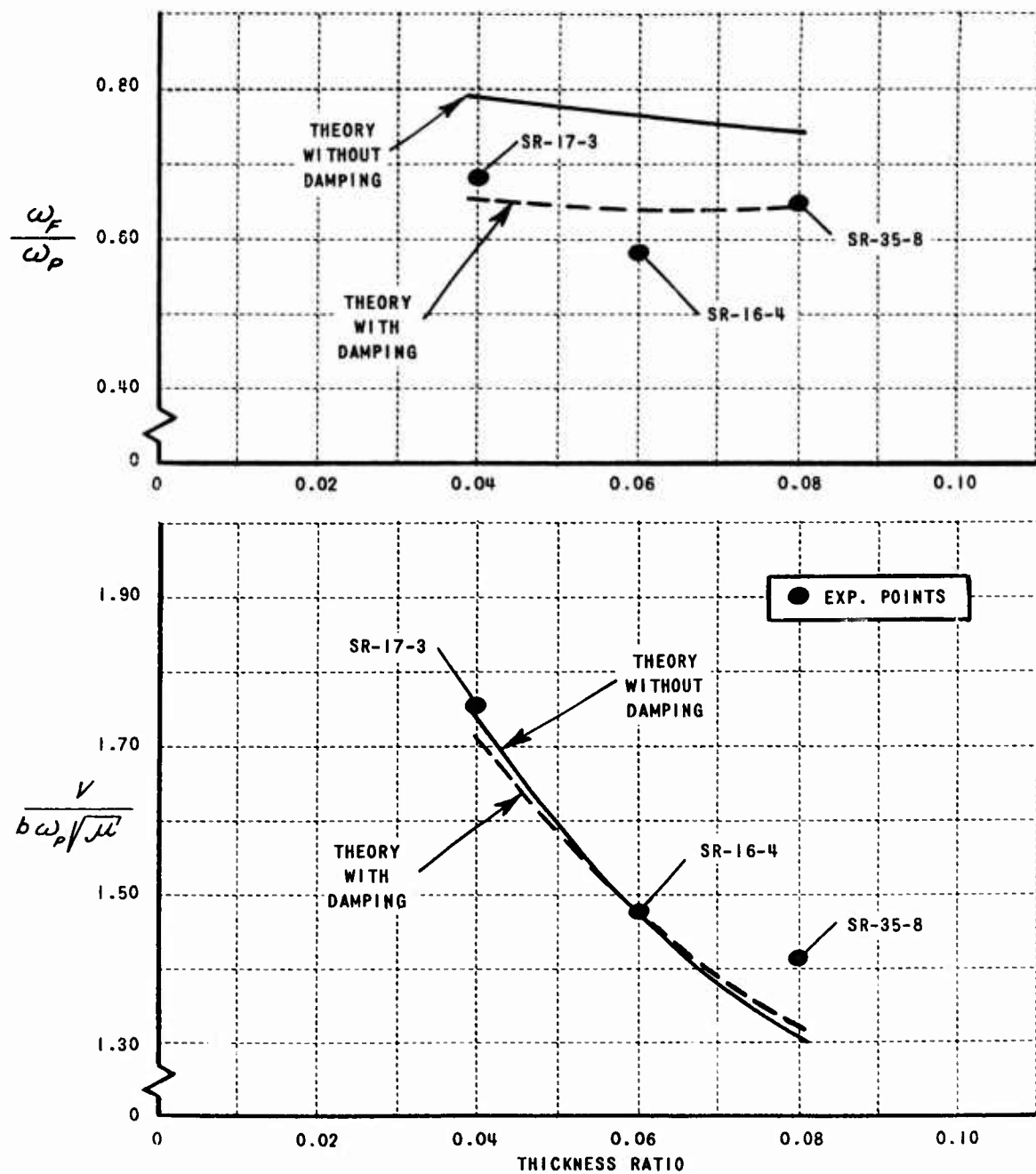


Figure 10 $\frac{\omega_F}{\omega_p}$ $\frac{V}{b\omega_p\sqrt{\mu'}}$ VS. THICKNESS RATIO
MACH NO. ≈ 5.0

CONFIDENTIAL

CONFIDENTIAL

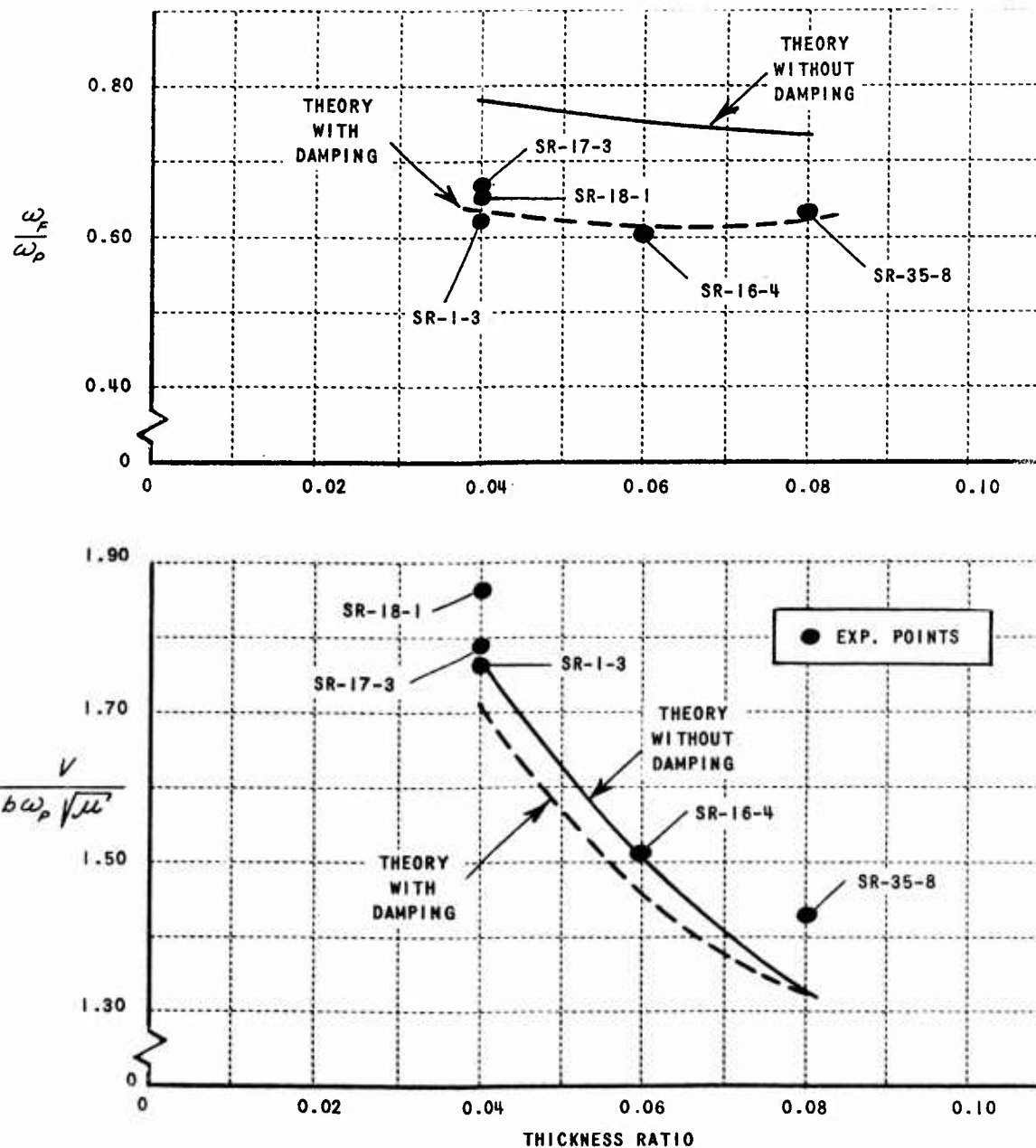


Figure 11 ω_F/ω_p & $V/b\omega_p\sqrt{\mu'}$ VS. THICKNESS RATIO,
MACH NO. $\cong 6.0$

CONFIDENTIAL

CONFIDENTIAL

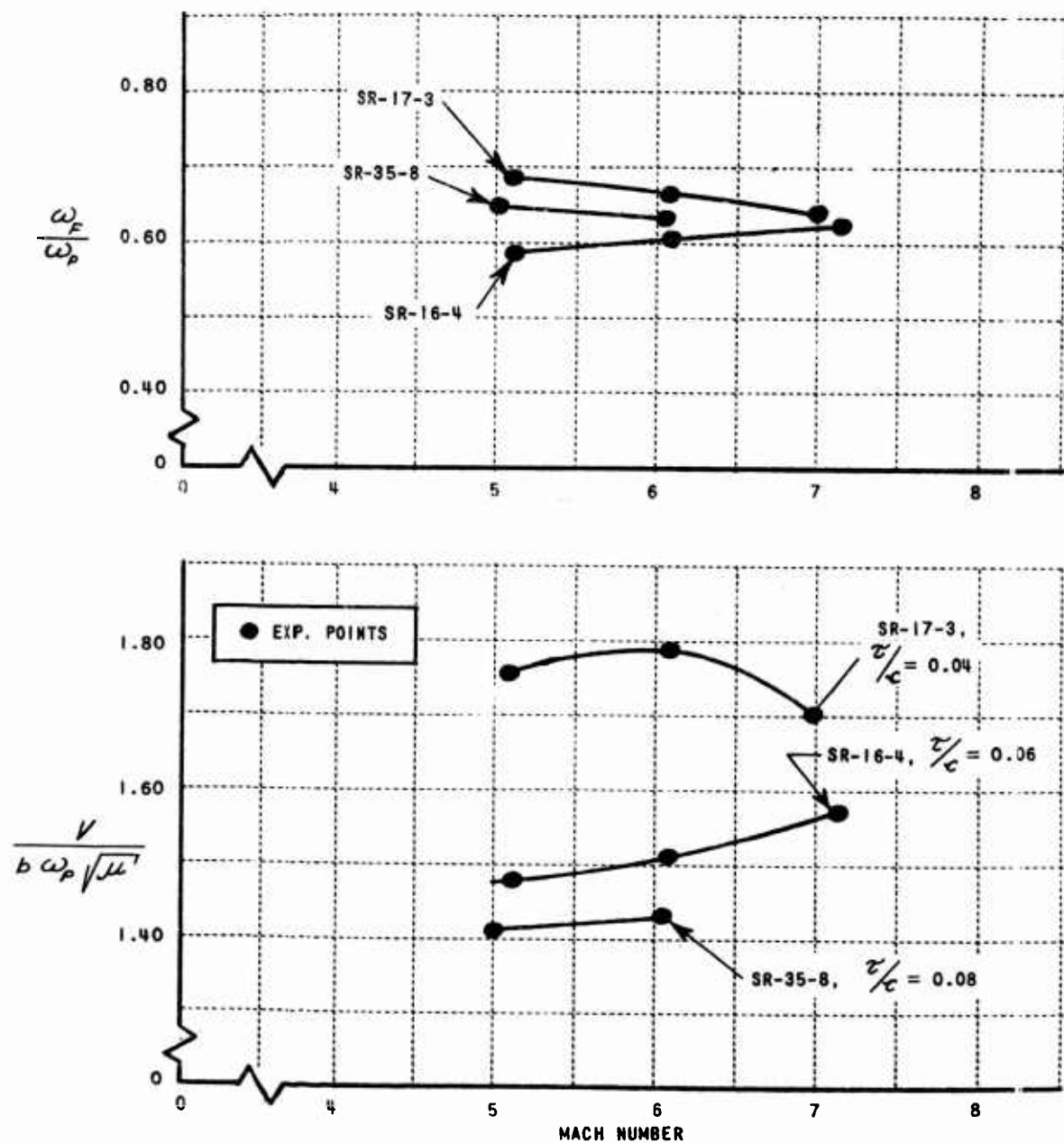


Figure 12 ω_F/ω_p & $V/b\omega_p\sqrt{\mu'}$ VS. MACH NUMBER FOR VARIOUS THICKNESS RATIOS, $\omega_r/\omega_p \approx 0.50$

CONFIDENTIAL